Sec1p directly stimulates SNARE-mediated membrane fusion in vitro

Brenton L. Scott, Jeffrey S. Van Komen, Hassan Irshad, Song Liu, Kirilee A. Wilson, and James A. McNew

Department of Biochemistry and Cell Biology, Rice University, Houston, TX 77251

Sec1 proteins are critical players in membrane trafficking, yet their precise role remains unknown. We have examined the role of Sec1p in the regulation of post-Golgi secretion in *Saccharomyces cerevisiae*. Indirect immunofluorescence shows that endogenous Sec1p is found primarily at the bud neck in newly budded cells and in patches broadly distributed within the plasma membrane in unbudded cells. Recombinant Sec1p binds strongly to the t-SNARE complex (Sso1p/Sec9c) as well as to the fully assembled ternary SNARE complex (Sso1p/Sec9c;Snc2p), but also binds weakly to free Sso1p. We used recombinant Sec1p to test Sec1p function using a well-characterized SNARE-mediated membrane fusion assay. The addition of Sec1p to a traditional in vitro fusion assay moderately stimulates fusion; however, when Sec1p is allowed to bind to SNAREs before reconstitution, significantly more Sec1p binding is detected and fusion is stimulated in a concentration-dependent manner. These data strongly argue that Sec1p directly stimulates SNARE-mediated membrane fusion.

Introduction

The growth and division of cells requires a regulated deposition of new plasma membrane. This is accomplished in part by the faithful delivery of Golgi-derived secretory vesicles by fusion with the plasma membrane. This seemingly simple membrane fusion event is responsible for a multitude of diverse biochemical processes such as the secretion of hormones, release of neurotransmitters, and the localization of a host of receptor proteins and most other integral membrane proteins to the plasma membrane.

Biological membrane fusion relies on proteins to drive the fusion reaction. The fusion of intracellular transport vesicles is mediated by a protein family collectively known as SNAREs (Sollner et al., 1993; Weber et al., 1998). SNARE proteins are operationally divided into two groups: those found primarily on the transport vesicle SNARE (v-SNARE), and those found primarily on the target membrane SNARE (t-SNARE). Although it is clear that SNAREs provide the mechanical force required for membrane fusion, it is also clear that they do not work alone in the cell.

The process of transport vesicle docking and fusion is tightly regulated. Regulatory proteins have been identified that interact with individual SNAREs as well as proteins that interact with the assembled SNARE complex (Ungar and Hughson, 2003). These include general regulatory proteins that likely function in all fusion reactions such as the Sec1/Munc18 (SM) family and the Rab family of small GTP-binding proteins (Pfeffer, 2001; Toonen and Verhage, 2003). In addition, there are a variety of compartment specific proteins such as those that have evolved specifically to regulate the speed and efficacy of synaptic transmission.

The mechanistic study of membrane fusion by the SNARE proteins has been aided tremendously by the development of a completely synthetic reconstitution system (Weber et al., 1998). This assay has been used to define the SNARE protein family as the primary driving force responsible for membrane merger (Weber et al., 1998), determine SNARE contributions to the specificity of membrane fusion (McNew et al., 2000a), address mechanistic questions and structure/function studies (McNew et al., 1999, 2000b; Parlati et al., 1999; Melia et al., 2002), as well as identify new functional SNARE complexes (Fukuda et al., 2000; Parlati et al., 2000, 2002; Paumet et al., 2001, 2004). More recently, this technique has been used to examine the role of potential fusion regulators such as synaptotagmin (Tucker et al., 2004), synaptic vesicle proteins (Hu et al., 2002), and in our case, Sec1p.

The SM family is a widely studied, yet incompletely understood group of proteins that have been shown to regulate membrane fusion (Gallwitz and Jahn, 2003; Toonen and Verhage, 2003). Most species contain between four and seven SM genes functioning at different transport steps. *Saccharomyces cerevisiae*

Correspondence to James A. McNew: mcnew@rice.edu

Abbreviations used in this paper: β-ME, β-mercaptoethanol; GSH, reduced glutathione; His_6-Sec1p, His_6-tagged Sec1p; OG, *n*-octyl-β-D-glucopyranoside; SM, Sec1/Munc18; t-SNARE, target membrane SNARE; v-SNARE, vesicle SNARE.

The Journal of Cell Biology, Vol. 167, No. 1, October 11, 2004 75–85
http://www.jcb.org/cgi/doi/10.1083/jcb.200405018

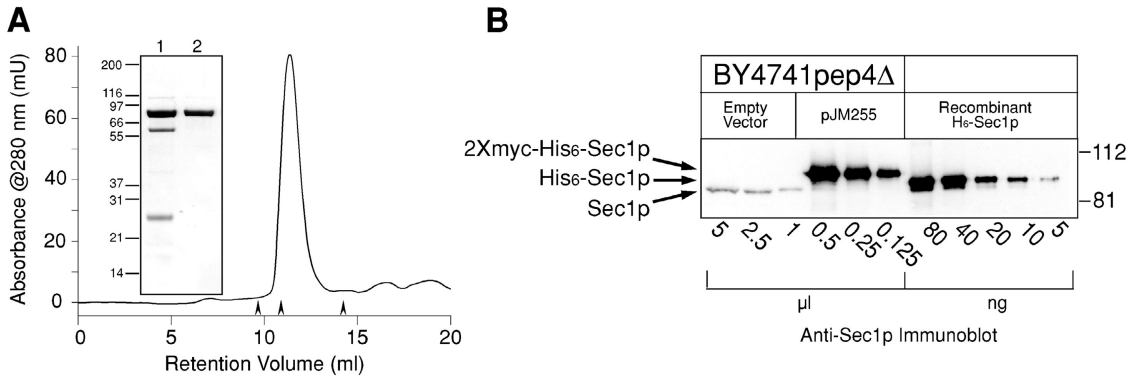

Figure 1. **Production of Sec1p and characterization of Sec1p antisera.** (A) Recombinant His_6-Sec1p production. Size exclusion chromatogram. His_6-Sec1p migrates as a single species and elutes slightly slower than BSA (67,000 D, middle arrowhead) on a Superose 12 (HR 10/30) column. Left arrowhead is 200,000 D (β-amylase) and the right arrowhead is 12,400 D (Cytochrome *c*). (Inset) Coomassie blue–stained gel of purified Sec1p. Lane 1 is a pooled fraction from metal chelate chromatography. This pool was further purified by ion-exchange chromatography, shown in lane 2. (B) Sec1p antibody production and yeast overexpression. The specificity of the polyclonal antisera is shown by detection of endogenous Sec1p in cytosolic extracts of the BY4741pep4Δ strain carrying the empty parent vector pYX223, and the detection of overexpressed Sec1p (2Xmyc-His_6-Sec1p, pJM255). The degree of overproduction is also measured with the Sec1p antisera in comparison to a dilution series of recombinant Sec1p from *E. coli*.

expresses four SM proteins: Sec1p functions at the plasma membrane (Novick et al., 1980; Carr et al., 1999); Sly1p regulates ER to Golgi transport (Ossig et al., 1991); Vps33p controls vacuolar traffic (Banta et al., 1990); and Vps45p operates in the TGN/endosomal system (Cowles et al., 1994; Dulubova et al., 2002). Genetic and biochemical studies of SM family members from different organisms and different transport steps suggest that Sec1 has both positive and negative effects on vesicle fusion. Loss of function mutations in SM family members are most often lethal and always lead to severe membrane fusion defects, suggesting that SM proteins have a required or positive role (Gallwitz and Jahn, 2003; Toonen and Verhage, 2003). Conversely, biochemical experiments show that neuronal Sec1 (n-Sec1) binds to the closed conformation of free Syntaxin1A likely preventing t-SNARE complex formation, suggesting that SM proteins may have a negative role (Yang et al., 2000). To complicate matters further, yeast Sec1p is reported to bind to the fully assembled SNARE complex (Carr et al., 1999).

Here, we report the first direct test of Sec1p function during membrane fusion. In vitro fusion reactions driven by the yeast exocytic SNAREs Sso1p, Sec9p, and Snc1/2p have been used to determine the effects of Sec1p on the rate or extent of membrane fusion. We document the production of recombinant Sec1p in bacteria and overexpression of Sec1p in *S. cerevisiae*. Recombinant Sec1p was used to generate pAbs allowing localization of endogenous Sec1p. Binding experiments to bead-bound SNAREs in detergent show that Sec1p binds to the t-SNARE complex (Sso1p/Sec9c), the fully assembled ternary SNARE complex (Sso1p/Sec9c; Snc2p) and weakly to free Sso1p. Functional reconstitution of t-SNARE (Sso1p/Sec9c) proteoliposomes with bound Sec1p strongly stimulates membrane fusion with Snc1p-containing proteoliposomes. Our results suggest that Sec1p may directly facilitate the formation of v-t-SNARE complexes between membranes, likely by directly affecting the t-SNARE complex.

Results

Sec1p production

One of the primary goals of this work was to determine the effect of adding Sec1p to an in vitro fusion assay containing reconstituted SNARE proteins in synthetic phospholipids. Sec1 family members have been notoriously difficult to prepare in recombinant form; however, we succeeded in producing soluble recombinant Sec1p in *E. coli.* A full-length NH_2-terminal His_6-tagged Sec1p (His_6-Sec1p) resulted in the best yield of soluble pure protein. Optimal conditions included coexpression with the *E. coli* chaperones GroEL and GroES (Yasukawa et al., 1995) and a 12-h induction at 25°C with low (0.2 mM) IPTG. Nickel affinity chromatography followed by ion exchange with Q-Sepharose resulted largely in a single protein by SDS-PAGE analysis (Fig. 1 A, inset). Recombinant Sec1p migrated as a single peak on size exclusion chromatography with a molecular size slightly more compact than the predicted 85,600 D molecular mass (Fig. 1 A). The purified protein has a tendency to aggregate and precipitate upon storage and repeated freeze-thaw cycles. Maintaining Sec1p concentrations below ~0.2 mg/ml minimized this problem.

Sec1p was also generated by overexpression in *Saccharomyces cerevisiae*. In contrast to other species, significant overexpression in *S. cerevisiae* had little or no deleterious growth effects. Increasing or decreasing the levels of ROP, the Sec1p homologue in *Drosophila*, results in a decrease of evoked and spontaneous neuro exocytosis (Wu et al., 1998). In *S. cerevisiae,* however, a 50–60-fold overexpression of 2Xmyc-His_6-tagged Sec1p (Fig. 1 B) had little or no effect on the overall growth rate of the yeast (178 min doubling time for wild-type versus 210 min doubling time for Sec1p overexpression). Based on Western blot comparisons to quantified recombinant Sec1p (Fig. 1 B), it is estimated that Sec1p makes up ~0.35% of the total soluble protein in this overexpression strain. Furthermore, the amount of Sec1p obtained in the extract was largely the same in the presence or absence of deter-

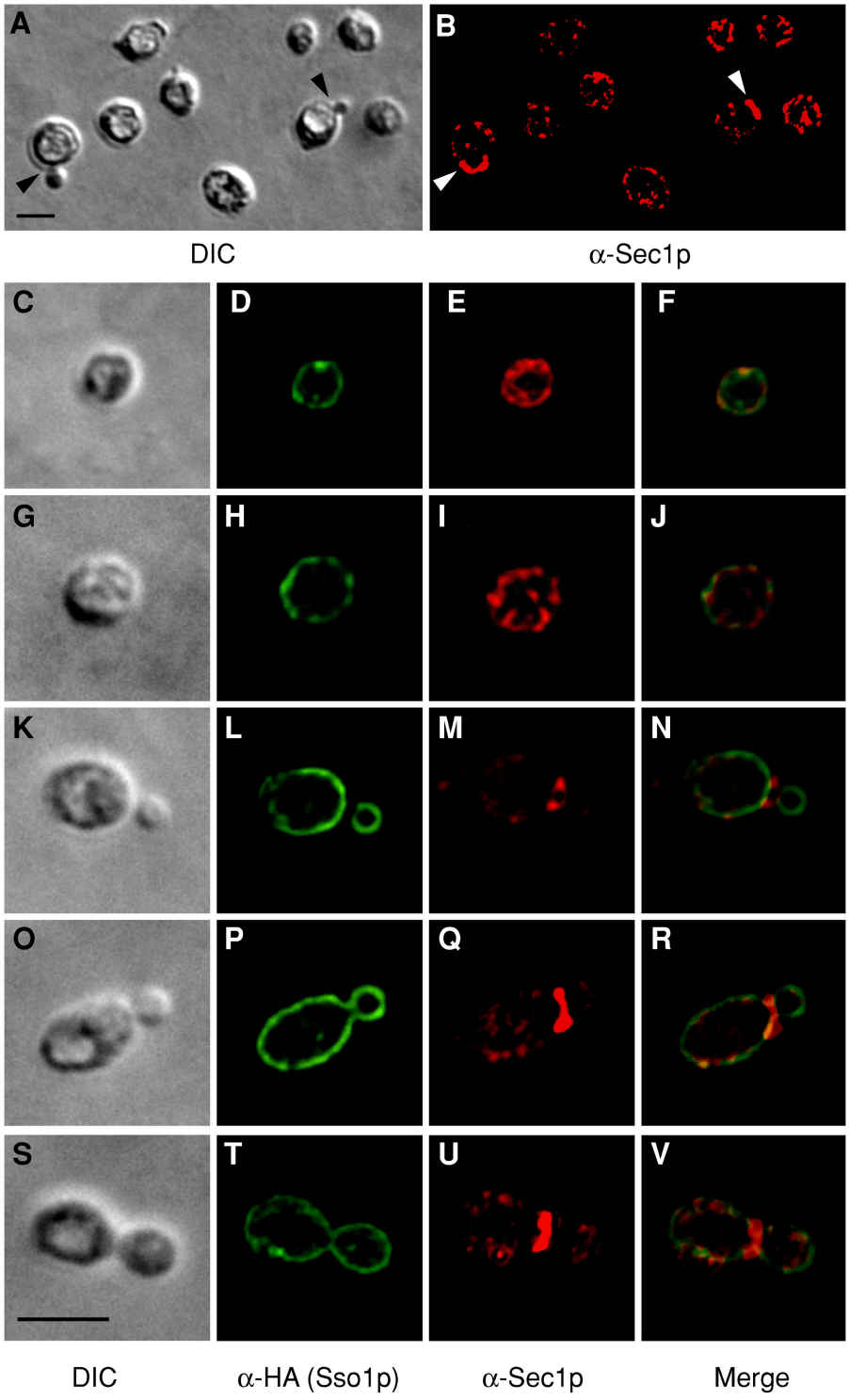

Figure 2. **Immunolocalization of endogenous Sec1p.** Sec1p localizes to patches on the plasma membrane. (A) Differential interference contrast (DIC) image of *S. cerevisiae*. (B) Endogenous Sec1p is imaged in the field of cells shown in A using a polyclonal anti-Sec1p antibody. Arrowheads denote newly emerged buds. (C–V) Individual cells in different stages of the cell cycle are imaged: Small, unbudded cells (C–J), small-budded cells (K–R), and a large-budded cell (S–V). DIC images (C, G, K, O, and S) and indirect immunofluorescence images are shown for each cell. Sso1p localization was determined by staining a HA-tagged Sso1p with anti-HA (D, H, L, P, and T). Endogenous Sec1p localization in individual cells is illustrated (E, I, M, Q, and U) and a merge of both Sso1p and Sec1p staining is imaged (F, J, N, R, and V). We determined that 71 ± 15% of endogenous Sec1p colocalizes with Sso1p-HA (n = 62 cells) when total cell area is examined. Bars, 5 μm.

gent (0.5% NP-40; unpublished data). The functionality of the NH_2-terminally tagged Sec1p was confirmed by tetrad dissection (unpublished data).

Endogenous Sec1p localizes throughout the plasma membrane

pAbs raised against recombinant Sec1p allowed us to determine the localization of endogenous Sec1p, which is predicted to be a soluble protein with no physical attachments to the membrane. Our analysis suggests that Sec1p is mostly localized to the plasma membrane and broadly distributed as patches throughout the plasma membrane (Fig. 2). This localization is very similar to the plasma membrane SNAREs Sso1p (Fig. 2, D, H, L, P, and T) and Sec9p (Brennwald et al., 1994). In fact, Sec1p significantly colocalizes with Sso1p (Fig. 2, F, J, N, R, and V). Although Sec1p is seen in all parts of the plasma membrane in unbudded cells (Fig. 2, E and I), it seems to be concentrated in the bud neck of newly budded cells (Fig. 2 B, arrowheads; Fig. 2, M, Q, and U).

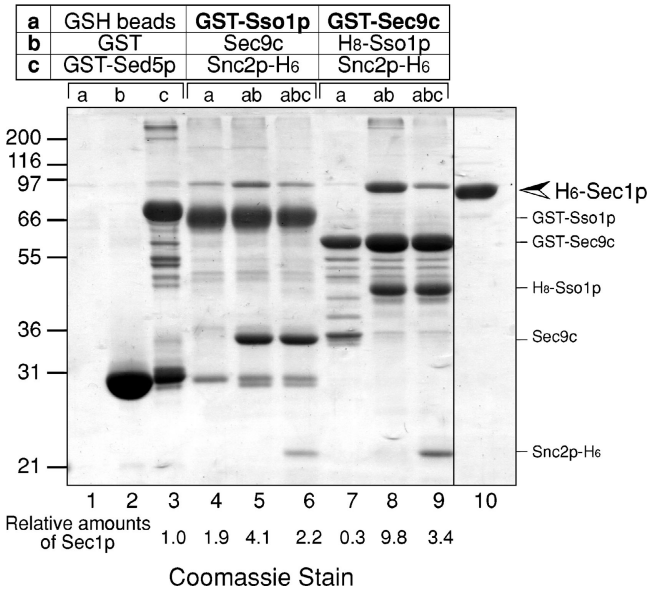

Figure 3. **Sec1p binds strongly to the t-SNARE complex (Sso1p/Sec9c) and the fully assembled ternary SNARE complex (Sso1p/Sec9c;Snc2p).** GST pull-down experiments were used to assess the degree of Sec1p binding to various SNAREs and SNARE complexes. The level of nonspecific binding was determined by incubation of recombinant Sec1p with protein-free GSH beads (lane 1), GST (lane 2), or GST-Sed5p (lane 3). The level of Sec1p binding to GST-Sed5p (which was approximately four times higher than either protein free beads or GST alone) was used as the background value for quantitative analysis. Sec1p binding to three SNARE species was analyzed: free t-SNARE (lanes 4 and 7), the binary t-SNARE complex (lanes 5 and 8) or the ternary SNARE complex (lanes 6 and 9). The three species were attached to glutathione beads via GST-Sso1p (lanes 4–6) or GST-Sec9c (lanes 7–9). Purified recombinant Sec1p (lane 10) is also shown (~1.4 μg, ~16 pmol). Sec1p binding was quantified by densitometry and is represented as fold above the GST-Sed5p background. Sec1p binds most significantly to the t-SNARE complex (lanes 5 and 8) as well as the ternary SNARE complex (lanes 6 and 9). A weaker association was also seen with the free monomeric SNAREs GST-Sso1p (lane 4). No binding to free GST-Sec9c (lane 7) was detected above background.

Recombinant Sec1p binds to t-SNARE complexes and the fully assembled ternary SNARE complex

Recombinant neuronal Sec1 binds to the closed conformation of Syntaxin1A (Misura et al., 2000; Yang et al., 2000), whereas Sec1p from a yeast cytosol extract has been reported to bind to the fully assembled ternary SNARE complex (Carr et al., 1999). To resolve these differences, we examined the binding characteristics of recombinant yeast Sec1p to various SNAREs and SNARE complexes. We used well-characterized GST pull-down assays where individual SNAREs or SNARE complexes were bound to glutathione agarose beads and roughly twofold molar excess amounts of recombinant Sec1p was added. Sec1p was allowed to bind for ~16 h at 4°C, and after extensive washing, the bound complexes were eluted by SDS sample buffer, resolved by SDS-PAGE and visualized by Coomassie blue staining. We examined complexes assembled on GST-Sso1p and GST-Sec9c (containing only the SNAP25 homologous portion of Sec9p). Three conditions were examined for Sec1p binding: free GST-SNARE, the t-SNARE complex, and the fully assembled ternary SNARE complex. Fig. 3 illustrates the results of a representative binding assay. Minimal amounts of Sec1p nonspecifically associated with reduced glutathione (GSH) resin (lane 1), GST (lane 2), or the Golgi SNARE Sed5p (lane 3). Specific Sec1p binding was detected to free GST-Sso1p (Fig. 3, 1.9-fold above the highest background, lane 4 vs. lane 3), but not to free GST-Sec9c (Fig. 3, lane 7). Binding of Sec1p to the t-SNARE complex (Fig. 3, lanes 5 and 8) was 4–10-fold more than background values. Significant binding of Sec1p to the ternary SNARE complex (Fig. 3, lanes 6 and 9) was also observed, strengthening a previous observation that an immunodetectable amount of Sec1p from cytosol associates with the fully assembled SNARE complex (Carr et al., 1999). We have now shown binding to the ternary SNARE complex at levels detected by Coomassie blue staining. Our data extend that observation to include detectable binding of Sec1p to the uncomplexed t-SNARE protein GST-Sso1p. Importantly, maximum Sec1p binding was detected to Sso1p/Sec9c t-SNARE complexes, suggesting that this is the preferred partner.

Binding of Sec1p to the ternary SNARE complex was consistently reduced compared with t-SNARE complex binding (Fig. 3, compare lane 5 vs. lane 6 and lane 8 vs. lane 9) suggesting that Snc2p may influence Sec1p binding when SNARE complexes are preassembled. To address this issue, we analyzed Sec1p (and Snc2p) binding under different experimental conditions. First, we conducted a binding experiment where all of the protein components were added simultaneously to GST-Sec9c bound resin (Fig. 4 A). Binary t-SNARE complexes (Fig. 4 A, lanes 1–4) or ternary SNARE complexes (Fig. 4 A, lanes 5–8) were formed in the presence of increasing concentrations (0, 0.25, 0.5, and 1.0 μM) of Sec1p. These results show that the presence of Sec1p does not affect the extent of t-SNARE complex formation or the extent of ternary SNARE complex formation. The overall degree of Sec1p binding is similar when SNARE complexes are preformed and Sec1p is in excess (Fig. 3, lanes 8 and 9) or when equal molar amounts of SNARE complexes form in the presence of Sec1p (Fig. 4 A, lanes 4 and 8).

Next, we asked if Snc2p could displace bound Sec1p as Snc2p engaged the t-SNARE complex during ternary SNARE complex formation (Fig. 4 B). GST-Sec9c/Sso1p t-SNARE complexes were formed on beads with (Fig. 4 B, lanes 5–8) or without (Fig. 4 B, lanes 1–4) bound Sec1p. These complexes were challenged with an increasing concentration of Snc2p in a one-, two-, or fourfold molar excess. Fig. 4 B illustrates that Snc2p forms an efficient ternary SNARE complex irrespective of the presence of Sec1p and does not significantly displace Sec1p from the t-SNARE complex.

Sec1p directly stimulates SNARE-mediated membrane fusion

Recombinant Sec1p was added to in vitro fusion assays to determine its effects on fusion. Fusion was modestly stimulated when recombinant Sec1p was mixed for 12–15 h at 4°C with proteoliposomes that contained the t-SNARE complex Sso1p/Sec9c before the addition of fluorescently labeled v-SNARE liposomes containing Snc1p (Fig. 5). Due to the low concentration of Sec1p (<0.2 mg/ml), we had to reduce the overall amount of t-SNARE containing liposomes in the fusion assay

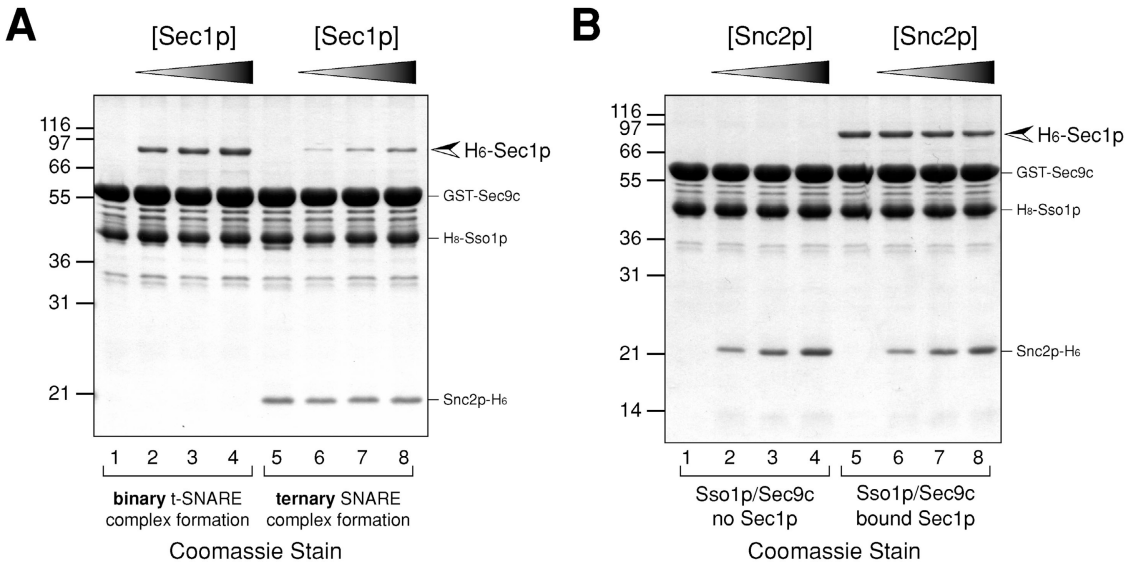

Figure 4. **Effect of Sec1p on SNARE complex formation.** (A) Binary t-SNARE complex and ternary SNARE complex formation is unaffected by Sec1p when all components are added simultaneously. GST-Sec9c was bound to resin and equimolar amounts of His_8-Sso1p, Snc2p-His_6, and increasing amounts of His_6-Sec1p (0, 0.1, 0.2, and 0.4 nmol) were added at the same time and incubated at 4°C for ~16 h. Bound complexes were resolved by SDS-PAGE and stained with Coomassie blue. (B) Snc2p can efficiently bind to Sec1p bound t-SNARE complexes without significant displacement of Sec1p. Increasing amounts of Snc2p (0, lane 1 and 5, 0.4 nmol lane 2 and 6, 0.8 nmol, lanes 3 and 7 and 1.6 nmol, lanes 4 and 8) were allowed to associate with preformed t-SNARE complex (Sso1p/Sec9c, lanes 1–4) or Sec1p bound t-SNARE complexes (Sec1p:Sso1p/Sec9c, lanes 5–8) for ~16 h at 4°C. Bound complexes were resolved by SDS-PAGE and stained with Coomassie blue.

and double the reaction volume. Even with these adaptations, we were unable to add Sec1p in excess of the t-SNARE complex. Sec1p was added at a molar ratio of ~0.7. Under these conditions, the fusion obtained with Sso1p/Sec9c;Snc1p with buffer added instead of Sec1p (Fig. 5, open circles) was roughly 0.75 rounds of fusion at 120 min. The presence of Sec1p stimulated fusion to ~1.0 round of fusion (Fig. 5, closed circles). The Sec1p mediated stimulation is SNARE dependent because soluble Snc2p completely inhibits fusion (Fig. 5, solid and dashed lines). The level of Sec1p stimulation was 39.3 ± 3.3% (mean ± SEM) above the background subtracted buffer controls for four independent preparations of Sec1p.

Sec1p modestly stimulates fusion when added directly to an in vitro fusion assay. Given that Sec1p binds to t-SNARE complexes in detergent (Figs. 3 and 4), we determined if similar Sec1p containing complexes could be reconstituted into liposomes. His_6-Sec1p was mixed with His_8-Sso1p or His_8-Sso1p/GST-Sec9c t-SNARE complexes in the presence of 0.6% octyl-glucoside for ~15 h at 4°C. The overall amount of t-SNARE complex protein added to the reconstitution was reduced to favor the ratio of Sec1p to t-SNARE complex. The detergent solutions were then used to resuspend a lipid film to form unlabeled t-SNARE proteoliposomes. Vesicles were isolated by flotation in a density gradient and analyzed for the presence of specifically bound Sec1p by SDS-PAGE and Coomassie blue staining (Fig. 6 A). We found that significant amounts of His_6-Sec1p were isolated with liposomes containing t-SNARE complexes (Fig. 6 A, lanes 2–5); whereas little or no Sec1p was isolated with liposomes containing free His_8-Sso1p (Fig. 6 A, lane 1) or protein free liposomes (not depicted).

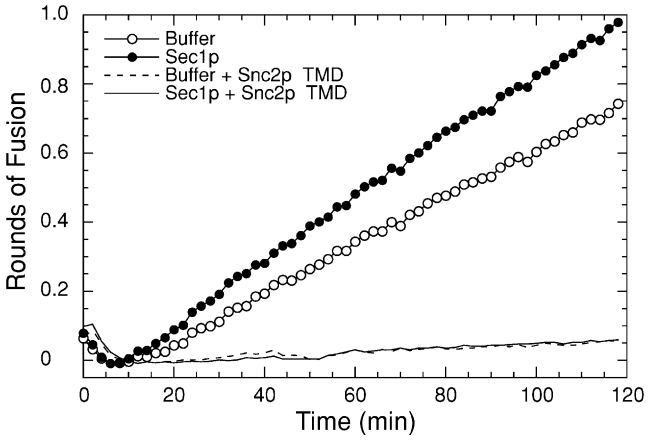

Figure 5. **Sec1p stimulates in vitro fusion.** Recombinant Sec1p was added to an in vitro fusion assay containing reduced levels of SNARE proteins. 10 μl of t-SNARE liposomes (Sso1p/Sec9c, ~19.5 μg, ~215 pmol of t-SNARE complex proteins, ~22.5 nmol lipid) was mixed with 85 μl of recombinant His_6-Sec1p (~12.8 μg, ~150 pmol, closed circles) or buffer A200 (open circles) for ~15 h at 4°C. 5 μl of Snc1p liposomes (~8.3 μg, 630 pmol Snc1p and 1.95 nmol lipid) were added and the NBD fluorescence measured for 2 h in a fluorescent plate reader at 37°C. The background values (solid and dashed lines) represent an inhibited reaction containing the same components as stimulated fusion reaction in addition to the soluble domain of Snc2p to inhibit vesicle fusion. The amount of fusion at 120 min was 0.98 rounds of fusion for the Sec1p stimulated curve (closed circles), 0.74 rounds of fusion for basal fusion (open circles), compared with an inhibited background of 0.05 rounds of fusion. This experiment was repeated three additional times using independent recombinant Sec1p purifications. The average stimulation observed of the four experiments was 39.3% ± an SEM of 3.3%. In addition, each sample was fused with protein free fluorescently labeled liposomes that showed a background fusion level of 0.059 rounds of fusion (not depicted).

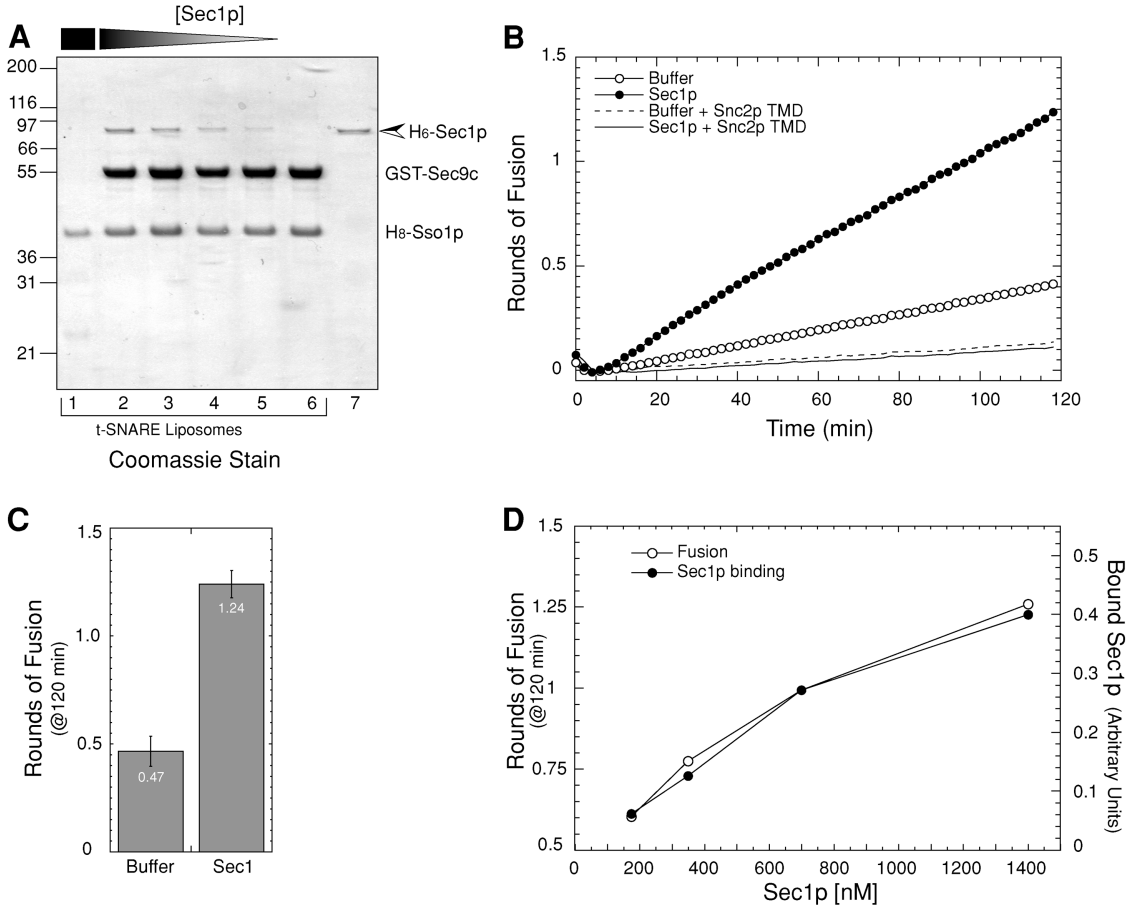

Figure 6. **SNARE-bound Sec1p strongly stimulates in vitro fusion.** A twofold dilution series of Sec1p was bound to t-SNARE complexes (Sso1p/Sec9c) in detergent solution before vesicle reconstitution. (A) Coomassie blue–stained gel of liposomes containing Sec1p bound t-SNARE complexes. Acceptor t-SNARE liposomes containing various amounts of bound His_6-Sec1p were resolved on a 10% Bis-Tris NuPAGE gel (Invitrogen) and stained with Coomassie blue. Lane 1 contains 15 μl of liposomes derived from a reaction containing His_8-Sso1p (~160 μg, ~4.7 nmol) and 60 μg (700 pmol) of His_6-Sec1p. Lanes 2–6 contains 10 μl of liposomes derived from reactions including His_8-Sso1p (~160 μg, ~4.7 nmol), GST-Sec9c (~430 μg, ~7.7 nmol) and decreasing amounts of Sec1p: lane 2, ~60, μg, ~700 pmol; lane 3, ~30 μg, ~350 pmol; lane 4, ~15 μg, ~175 pmol; and lane 5, ~7.5 μg, ~88 pmol. Lane 6 contained no Sec1p. Lane 7 contains 0.6 μg (~7 pmol) of recombinant His_6-Sec1p. (B) Kinetic fusion graph of Sec1p stimulated fusion. Vesicles (45 μl) containing t-SNARE complexes without Sec1p (open circles, ~13 μg, 145 pmol Sso1p/Sec9c and 42 nmol lipid) and t-SNARE vesicles containing the highest amount of bound Sec1p (closed circles) were mixed with fluorescently labeled vesicles containing the v-SNARE Snc1p (5 μl, ~8.3 μg, 630 pmol Snc1p and 1.95 nmol lipid) and incubated for 120 min at 37°C in a standard fusion reaction. The extent of fusion is represented as rounds of fusion, measured as fold lipid dilution in the reaction. The background values (solid and dashed lines) represent an inhibited reaction containing the same components in addition to the soluble domain of Snc2p to inhibit vesicle fusion. The amount of fusion at 120 min was 1.32 rounds of fusion for the Sec1p stimulated curve (closed circles), 0.42 rounds of fusion for basal fusion (buffer, open circles), and the inhibited fusion background, 0.1 rounds of fusion. Sec1p stimulated fusion ~3.8-fold in this experiment after background subtraction. (C) Average fold stimulation caused by Sec1p. The amount of stimulation by Sec1p was examined using four independent preparations of recombinant His_6-Sec1p. This histogram shows that His_6-Sec1p stimulates fusion by 2.7-fold on average. The mean ± SEM are represented after the subtraction of an average background of 0.105 rounds of fusion. (D) Sec1p titration showing stimulation is concentration dependent. The extent of fusion observed at 120 min and the amount of Sec1p binding detected to t-SNARE liposomes is represented for independent in vitro fusion experiments relative to the amount of Sec1p added to the reaction. Rounds of fusion at 120 min are shown on the left y axis (open circles) and the amount of Sec1p binding (relative to His_8-Sso1p) is quantified on the right y axis (closed circles). Both values are plotted relative to the concentration of Sec1p added to the reaction (nM). The binding values for Sec1p were determined by quantifying the gel shown in Fig. 6 A.

We next determined the effect of bound Sec1p on SNARE-mediated fusion. Fig. 6 B shows a kinetic fusion reaction with the His_8-Sso1p/GST-Sec9c t-SNARE complex with Sec1p bound or without Sec1p (buffer control). The highest concentration of bound Sec1p (Fig. 6 B, closed circles) stimulated fusion roughly threefold over the buffer control (Fig. 6 B, open circles). Soluble Snc2p inhibited fusion in all cases (Fig. 6 B, solid and dashed line) confirming that the Sec1p mediated stimulation is SNARE dependent. Stimulation by Sec1p was examined for four independent preparations of recombinant Sec1p, with an average stimulation by Sec1p of 2.7-fold (Fig. 6 C).

The amount of Sec1p bound relative to Sso1p is quantified in Fig. 6 D. At the highest concentration of added Sec1p (Fig. 6 A, lane 2, ~1.4 μM), the Sec1p band is roughly 40% of the Sso1p band. This corresponds to ~16% of the Sso1p containing bound Sec1p when differences in molecular weight are taken into consideration. Although Sec1p binding is substoichiometric, fusion stimulation is concentration dependent. When the levels of Sec1p are increased in the binding reaction, more Sec1p is seen associating with the SNARE liposomes and a proportional increase in fusion is also observed (Fig. 6 D). These data strongly argue that

Sec1p directly stimulates SNARE-mediated membrane fusion in vitro.

Discussion

Temperature-sensitive mutants in Sec1p were isolated in the original *sec* screen almost 25 yr ago (Novick et al., 1980). Since that time, the molecular analysis of vesicle docking and fusion has identified SNAREs as the protein machinery that drives membrane fusion and characterized many of the proteins that provide spatial control such as the exocyst and Sec3p (TerBush et al., 1996; Finger et al., 1998). However, the precise role of Sec1p has remained elusive.

We have examined the role of Sec1p in the process of SNARE-mediated membrane fusion in vitro. For this work, we have generated recombinant Sec1p expressed in bacteria (Fig. 1). In vitro binding experiments in detergent illustrate that recombinant Sec1p binds strongly to the preassembled t-SNARE complex (Sso1p/Sec9c) as well as the ternary SNARE complex (Sso1p/Sec9c;Snc2p). We also show an association with free Sso1p for the first time (Fig. 3).

Although Sec1p and n-Sec1 function in a compartmentally analogous transport event, their primary mechanism of action appears to be different. It is clear that neuronal Sec1 forms a strong complex with Syntaxin1A and this binding selects the closed conformation of Syntaxin1A and prevents further SNARE complex assembly. This mode of action suggests that n-Sec1 may serve as a negative regulator. (Dulubova et al., 1999; Yang et al., 2000). However, yeast Sec1p favors binding to the t-SNARE complex over the free syntaxin subunit or the fully assembled SNARE complex. This difference adds another level of complexity to the general function of SM proteins.

Because Sec1p preferentially binds to the t-SNARE complex (Fig. 3), we suggest that Sec1p functions to promote the reactivity of this complex. The available structural data of the yeast t-SNARE complex suggests that a COOH-terminal portion of Sso1p remains unstructured in the t-SNARE complex but gains structure when Snc1p binds (Fiebig et al., 1999). A potential function for Sec1p association could be to induce a conformational change that would structure the COOH-terminal portion of the Sso1p H3 domain. This is an appealing location given the contact of n-Sec1p with Syntaxin1A (Misura et al., 2000). A fully helical H3 domain would make v-SNARE zippering much more favorable. Although our binding studies show that the presence of bound Sec1p does not increase the extent of Snc2p binding (Fig. 4), it may provide a kinetic advantage that would be undetected in this analysis.

The effect of Sec1p binding was directly tested in an in vitro fusion assay. Fusion is moderately stimulated when recombinant Sec1p is added to a conventional in vitro fusion reaction containing the plasma membrane SNAREs Sso1p, Sec9c, and Snc1p (Fig. 5). However, when Sec1p was prebound in detergent before reconstitution, Sec1p stimulates fusion 2–3-fold compared with t-SNARE complexes that lack bound Sec1p (Fig. 6). Stimulation of fusion by Sec1p is concentration dependent and completely inhibited by soluble Snc2p. These results demonstrate that the presence of Sec1p significantly enhances SNARE-mediated membrane fusion in vitro and is the first in vitro evidence to show a functional consequence of SM protein binding.

Recombinant Sec1p was also used to generate pAbs that were used to localize endogenous Sec1p by indirect immunofluorescence. Previous studies have shown that GFP Sec1p was localized to sites of active growth, namely the bud tip in newly budded cells and the bud neck in larger budded cells closer to cytokinesis (Carr et al., 1999). This localization was more pronounced in certain *sec* mutants at the nonpermissive temperature (Grote et al., 2000) or mutations in Sso1p that favor t-SNARE complex formation (Munson and Hughson, 2002). No general plasma membrane localization was detected with GFP-Sec1p. Based on the observation that Sec1p binds to the assembled SNARE complex, GFP-Sec1p has been used a marker of SNARE complex formation in vivo because its localization has been linked to sites of active secretion (Grote et al., 2000; Munson and Hughson, 2002).

We find, looking at endogenous protein in fixed cells, that Sec1p shows a relatively uniform distribution throughout the plasma membrane (Fig. 2, E and I), similar to the plasma membrane t-SNARE component Sso1p (Fig. 2, D and H), though this is not likely due to a physical association of Sec1p with Sso1p alone on the membrane. We also see Sec1p concentrated at the bud neck at all stages of the cell cycle (Fig. 2, C–V), even in newly emerged buds (Fig. 2 B). Several possibilities could be suggested to explain the apparent differences between our localization and that of published reports (Carr et al., 1999; Grote et al., 2000; Munson and Hughson, 2002). GFP-Sec1p could potentially bind to different proteins or SNARE conformations than endogenous Sec1p or perhaps the NH_2-terminal GFP prevents association with the factors that provide general plasma membrane staining. We are currently examining this and other possibilities to account for the observed differences.

How do SM proteins regulate membrane fusion? SM proteins likely operate by binding to one or all of the three SNARE (complex) structural intermediates. These SM protein interaction modes include: (1) free syntaxin binding; (2) t-SNARE complex binding; and (3) fully assembled SNARE complex binding. All of these modes depend on a syntaxin as the common denominator. These different modes of binding likely generate different functional consequences. SM protein binding to a free syntaxin provides a negative regulatory function at the plasma membrane (n-Sec1/Syntaxin1A), but not on internal membranes (Sly1p/Sed5p, Sly1p/Ufe1p, or Vps45p/Tlg2p). This difference can be attributed to the specific way in which the SM protein interacts with the syntaxin partner. For example, n-Sec1 binds and stabilizes the closed conformation of Syntaxin1A, which precludes further SNARE complex formation, namely SNAP25 association (Yang et al., 2000); however, Sly1p and Vps45p interact with the extreme NH_2 terminus of their respective syntaxin (Dulubova et al., 2002; Yamaguchi et al., 2002) which allows further SNARE associations. Sec1p also binds, albeit weakly, to free Sso1p (Fig. 3), suggesting that mode 1 may occur in yeast although the functional consequences of this binding (if any) remain to be determined.

Sec1p binding to the t-SNARE complex (mode 2) stimulates fusion, providing a positive regulatory function (Figs. 3 and 6). The binding of other SM proteins to t-SNARE complexes has not been addressed. SM protein binding to the fully assembled SNARE complex (mode 3) occurs for Sec1p (Fig. 3) and Sly1 (Peng and Gallwitz, 2002), although the functional consequences for this interaction mode are not clear. This binding mode may favor trans-SNARE complex assembly (Kosodo et al., 2002), or be involved in SNARE recycling (Carr et al., 1999; Kosodo et al., 2003).

We suggest that all SM proteins may have the capacity to interact in all three modes. Different organisms as well as different trafficking steps within an organism may favor one mode over the others. For example, neurons may have amplified mode 1, whereas yeast use mode 2 as the primary function for the plasma membrane SM protein.

Thinking about SM protein function in this broader context may help to explain apparent experimental discrepancies in different systems seen with overexpression of SM proteins. Overexpression of ROP in *Drosophila* (Wu et al., 1998) or Munc18c in adipocytes (Thurmond et al., 1998) causes an inhibition of neurosecretion and GLUT4 vesicle fusion, respectively. Similarly, microinjection of squid sec1 (or sec1 peptides) in squid giant axons (Dresbach et al., 1998) or Munc18c peptides in adipocytes (Thurmond et al., 2000) inhibits vesicle trafficking. However, overexpression of Munc18-1 in chromaffin cells stimulates secretion of large dense core vesicles (Voets et al., 2001). Yet another study suggests that overexpression of Munc18-1 in PC12 cells or chromaffin cells is without effect (Graham et al., 1997). We also find that overexpressing Sec1p does not affect yeast growth (unpublished data), although we did not examine secretion directly. In the cases where secretion was decreased by increasing SM protein levels, the free syntaxin binding mode (mode 1) likely predominates and this binding probably prevents further SNARE complex assembly. In the cases where secretion is stimulated or unaffected, a different binding mode, likely mode 2, is more prevalent.

Genetic evidence also supports a model that the same SM protein can provide differential function. Four point mutations in the *Drosophila* SM protein ROP have been characterized. Two of these mutations (H302Y and D45N) show a decrease in evoked and spontaneous neurotransmission whereas the other two (P254S and R50C) have the opposite effect, an increase in neurotransmitter release (Wu et al., 1998). The latter two mutants may be impaired in mode 1 binding which would be seen as a relief of inhibition or a stimulation whereas the former could be impaired with either mode 2 or 3.

Our new results help to place the complicated function of the SM proteins into a new conceptual framework which may explain the apparently contradictory results. Further experiments will be required to test additional predictions of this work such as a reexamination of the binding properties of other SM protein family members.

Materials and methods

DNA constructs

Sec1p plasmids. pJM146 is a bacterial expression vector coding for His_6-Sec1p. The *SEC1* gene was generated by PCR using *S. cerevisiae* genomic DNA as a template and the oligos 124 and 125 (Table I). The *SEC1* gene was cut with NdeI and BamHI and ligated into pET15b (Novagen) cut with the same enzymes.

pJM250 is a yeast expression vector coding for His_6-Sec1p driven by the GPD promoter. An ~2,376-bp XbaI–BamHI fragment containing His_6-Sec1p was cut out of pJM146 and ligated into p426-GPD (Mumberg et al., 1995) cut with SpeI and BamHI.

pJM254 is a yeast expression vector coding for His_6-Sec1p driven by the GAL1 promoter. An ~2,366-bp NcoI–HindIII fragment containing His_6-Sec1p was cut out of pJM250 and ligated into pYX223 (Novagen) cut with the same enzymes. Note that Sec1p contains its native stop codon before the HA tagged coded by pYX223.

pJM255 is a yeast expression vector coding for 2Xmyc-His_6-Sec1p driven by the GAL1 promoter. A double-stranded oligo (158 and 159) were annealed and ligated into pJM254 cut with NcoI. Two copies of the double-stranded oligo were incorporated into pJM255. The 46–amino acid NH_2-terminal tag is MGEQKLI SEEDLYMGEQ KLISEEDLYM GSSHHHHHHS SGLVPRGSH.

Sso1p plasmids. pJM290 is a yeast expression vector coding for Sso1p-HA driven by the *GAL1-10* promoter. The *SSO1* gene was generated by PCR from *S. cerevisiae* genomic DNA as a template using oligos 41 and 178. The PCR fragment was digested with BamHI and MluI and ligated in pYX223 (Novagen) cut with the same enzymes.

pJM355 is a yeast expression vector coding for Sso1p-HA under the transcriptional control of the *SSO1* promoter. The ~933-bp *SSO1* fragment was generated by digesting pJM290 with EcoRI and XhoI. The ~496-bp fragment containing the 5′ untranslated region of *SSO1* was PCR amplified from *S. cerevisiae* genomic DNA as a template with oligos 216 and 217. The ~310-bp fragment containing the 3′ untranslated region of *SSO1* was PCR amplified from *S. cerevisiae* genomic DNA as a

Table I. **Oligonucleotides**

Oligo no.	Oligo name	Sequence
38	Sso1-1	CGGAATTCATGAGTTATAATAATCCGTACC
41	Sso1-4	GAGATATCCTCGAGACGCGTTTTGACAACAGCTGGG
124	Sec1-Bam	GCGGATCCTCATTTATCATGGTGAGATTTTC
125	NdeI-Sec1	CCCCATGGGCCATATGTCTGATTTAATTGAATTACAGAGG
126	Bam-Sec9	GCGGATCCATGGGATTAAAGAAATTTTTTA
127	Sec9stop-Xho	GCGGATCCCTCGAGCTATCTGATACCTGCCAACCTGTTG
158	Myc top	CATGGGAGAACAAAAACTTATTTCTGAAGAAGACTTGTA
159	Myc Bottom	CATGTACAAGTCTTCTTCAGAAATAAGTTTTTGTTCTCC
178	Sso1-13	GGGGATCCTATGAGTTATAATAATCCGTACC
216	Sso1-15	GGGAGCTCGCTTAATGGACTTCCTGGAGGAGG
217	Sso1-16	CGTCTAGAGATTTGTTTCTATTTTTAATTGCC−
218	Sso1-17	GCCTCGAGTAATTCCAACTATTTTCTATATTTC
219	Sso1-18	CCGGTACCGAGGTAGCATGTGAAAACGCGGGAG

template with oligos 218 and 219. All of these fragments were assembled into pRS424, a *TRP1-2* μm plasmid (Sikorski and Hieter, 1989)

pJM82 is a bacterial expression vector coding for Sso1p-His_6. The 892-bp *SSO1* gene was generated by PCR using *S. cerevisiae* genomic DNA as a template with oligos 38 and 41. This fragment was digested with EcoRI and XhoI and ligated into pET24 (Novagen)

pJM87 is a bacterial expression vector coding for GST-Sso1p. The *SSO1* ORF was cut out of pJM82 by digesting with EcoRI and XhoI and ligated into pGEX 4T-1. Note that this plasmid uses a stop codon in pGEX 4T-1 and generates seven additional amino acids (LERPHRD) coded by the vector sequence after the transmembrane domain of Sso1p.

Expression and purification of proteins in *E. coli*

Unless otherwise noted, all proteins were induced at 0.2 mM IPTG at mid-late log phase (OD of 0.6–0.8). Cells were lysed using an Emulsiflex-C5 high pressure homogenizer (Avestin). Lysate was clarified by centrifugation at 100,000 g_{max} for 1 h at 4°C and stored at −80°. Clarified lysate was further purified by nickel affinity chromatography for His-tagged proteins or GST affinity chromatography for GST-tagged proteins.

GST-tagged proteins

All GST-tagged proteins were expressed in DH5α (GIBCO BRL) *E. coli*. GST-Sed5p (pJM22), GST-Sec9c (BB442), and GST-Snc2ΔTMD (BB465a) were expressed and purified as described previously (McNew et al., 1998, 2000b). GST-Sec9c was further purified for use in the GST pull-down assay by ion exchange on Q-Sepharose high performance resin in buffer A50 (25 mM Hepes-HCl pH 5.1, 50 mM KCL, 10% glycerol), 1 mM DTT. Contaminant proteins bound and the flow through contained GST-Sec9c. Untagged Sec9c. Extract containing GST-Sec9c was bound to glutathione-agarose for 1 h at 4°C, washed with buffer A400 (25 mM Hepes-KOH, pH 7.4, 400 mM KCL, 10% glycerol [wt/vol]), resuspended in 1.5 ml of buffer A400, and cleaved with 8 U of thrombin (T1063; Sigma-Aldrich) for 120 min at 25°C to release soluble untagged Sec9c at ∼0.8 mg/ml for use in GST pull-down assays (Fig. 3). Thrombin activity was inhibited by the addition of aminoethybenzenesulfonyl fluoride to a final concentration of 10 mM.

GST-Sso1p (pJM87) was expressed in 2XYT media and induced at 37°C for 4 h. Protein was purified by GST-affinity chromatography as described previously (McNew et al., 2000a), except that cells were lysed with 1% Triton X-100 and protein eluted with 1% *n*-octyl-β-D-glucopyranoside (OG) and a low salt concentration of 50 mM KCl. GST-Sso1p protein was further purified by ion-exchange where GST-Sso1p was bound to a 1-ml Q-Sepharose column in buffer A50, pH 7.4, 2 mM β-mercaptoethanol (β-ME), 1% OG, and eluted with a linear 15-column vol KCl gradient from 50 to 1,000 mM with 1% OG. Peak fractions were pooled at ∼0.58 mg/ml with a final yield of ∼1.16 mg/four liters *E. coli* culture. GST was expressed in 2XYT media, induced at 37°C for 4 h and purified as described previously (McNew et al., 2000a) except that 100 mM KCL was used.

HIS-tagged proteins

Unless otherwise noted, all His-tagged proteins were expressed in BL21 (DE3) (Novagen) *E. coli* cells. His_8-Sso1p (pJM88-1), Snc2p-His_6 (pJM81-2), and Snc1p-His_6 (pJM90-1) were expressed and purified by nickel affinity chromatography as described previously (McNew et al., 2000a).

We produced His_6-Sec1p (pJM146) by coexpression with pTGroE (GroEL/GroES; a gift from S. Ishii, University of Tsukuba, Ibaraki, Japan; Yasukawa et al., 1995). Protein expression in Superbroth media was induced for ∼12 h at 25°C. Cells were lysed in buffer A200 (25 mM Hepes-KOH, pH 7.4, 200 mM KCl, 10% [wt/vol] glycerol), 2 mM β-ME and 1 complete protease inhibitor tablet. Soluble Sec1p was bound to a Ni^{2+}-chelating column in buffer A200, 2 mM β-ME, washed with buffer A200, 2 mM β-ME, 20 mM imidazole and eluted with a linear 20-column vol imidazole gradient from 20 to 500 mM using the AKTA prime purification system (Amersham Biosciences). Peak fractions were pooled and dialyzed overnight at 4°C against four liters of dialysis buffer (25 mM Tris-HCl, pH 8.0, 200 mM KCl, 10% glycerol), 1 mM DTT. Sec1p was further purified by ion exchange chromatography where Sec1p (6–10 ml) was mixed with 1 ml Q-Sepharose high performance resin (Amersham Biosciences) for 30 min at 4°C. Contaminant proteins bound and the flow through contained high purity Sec1p (Fig. 1 A, inset, lanes 1 and 2). 12 liters of *E. coli* culture yielded 1–10 mg of Sec1p solution. SDS-PAGE and size exclusion chromatography were used to analyze protein purity and size. Gel filtration over a Superose 12 column (HR10/30) using an AKTA FPLC (Amersham Biosciences) in buffer A200 at 1 ml/min illustrated that His_6-Sec1p eluted as a single peak with a size consistent with monomeric His_6-Sec1p. Gel filtration experiments were calibrated with β-amylase (200 kD), BSA (67 kD), and Cytochrome *c* (12.4 kD).

Sec1p overexpression yeast extract

2Xmyc-His_6-Sec1p in the pYX223 vector (pJM255), or the empty pYX223 vector as a control, was transformed into *S. cerevisiae* BY4741pep4Δ (MATa, his3Δ1, leu2Δ0 met15Δ0, ura3Δ0, pep4::kanMX4) cells (JMY228). Cells were grown to mid-log phase (OD ∼1.0) at 30°C in synthetic complete media lacking histidine, containing 2% (wt/vol) raffinose and 2% (wt/vol) galactose, lysed using an Emulsiflex-C5 high pressure homogenizer buffer A200, 2 mM β-ME (±0.5% NP-40) and clarified by centrifugation at 100,000 g_{max} for 1 h at 4°C.

Antibody production

The polyclonal anti-Sec1p antibodies (RC57 and RC58) were generated by Cocalico Biologicals, Inc. in rabbits immunized with recombinant Sec1p. Initial injections consisted of 200 μg/rabbit, followed by 100 μg/rabbit boost injections. Antisera at a 1:5,000 dilution in TBS with 1% Tween-20 was used for detection of Sec1p in conjunction with a 1:10,000 dilution in Tween-20 of secondary antibody goat anti–rabbit HRP (Pierce Chemical Co.). RC57 antisera was used throughout this work.

General reconstitution procedure

SNARE proteins were reconstituted as described previously (Scott et al., 2003). The t-SNAREs (Sso1p/Sec9c) were reconstituted into unlabeled lipid, and the v-SNARE (Snc1p) was reconstituted into labeled lipid containing NBD and rhodamine (Scott et al., 2003).

GST pull-down assay

For Fig. 3, GST-tagged proteins; GST-Sso1p (∼480 pmoles), GST-Sec9c (∼500 pmoles), GST-Sed5p (∼1 nmole) or GST alone (∼1 nmole) in buffer A400D (buffer A400 containing 1% Triton X-100, total volume of 100 μl) were bound to glutathione agarose beads for 1 h at 4°C. Unbound protein was removed by washing five times with 0.5 ml buffer A400D. To form t-SNARE complexes the appropriate partner SNARE was added in threefold molar excess, maintaining a final concentration of 1% Triton X-100, untagged Sec9c (∼1.5 nmoles, 55 μl), and His_8-Sso1p (∼1.6 nmoles, 20 μl). To form ternary SNARE complexes Snc2p-His_6 was added in twofold molar excess (∼0.9 nmoles, 15 μl). The total volume added was adjusted to 100 μl with buffer A400D. SNARE complexes were formed by incubation at 4°C for ∼16 h. Negative controls, GST alone or GST-Sed5p were mixed with buffer only.

SNARE complexes were washed five times with 0.5 ml buffer A200D (buffer A200 containing 1% Triton X-100). His_6-Sec1p protein (0.8 nmoles, 125 μl) was added to bound SNAREs maintaining a final concentration of 1% Triton X-100, and allowed to bind for ∼16 h at 4°C. The complexes were washed five times with 0.5 ml buffer A200D to remove unbound Sec1p. The proteins bound to glutathione agarose beads were eluted with 20 μl SDS sample buffer (125 mM Tris-HCL, pH 6.8, 50% [vol/vol] glycerol, 4% [wt/vol] SDS, 5% [vol/vol] β-ME, and 0.01% [wt/vol] bromophenol blue) and approximately equal amounts of bound GST-tagged proteins analyzed by SDS-PAGE and Coomassie blue (R250) staining.

For Fig. 4 A, GST-Sec9c (∼180 μg, ∼3.2 nmole) was bound to 100 μl of packed GSH beads equilibrated in buffer A400D for 1 h at 4°C in 200 μl total volume. Unbound proteins were removed by five, 0.5 ml washes with buffer A200D. Eight equal aliquots (12.5 μl of packed beads) were distributed in 0.5 ml microcentrifuge tubes. Four samples were used to analyze t-SNARE complex formation by adding His_8-Sso1p (0.4 nmol) and increasing amounts of Sec1p (0, ∼0.1, ∼0.2, or ∼0.4 nmoles). The remaining four samples were used to analyze ternary SNARE complex formation by adding His_8-Sso1p (0.4 nmol), Snc2-His_6 0.4 nmol) and increasing amounts of Sec1p (0, ∼0.1, ∼0.2, or ∼0.4 nmoles). The total volume was adjusted to 300 μl with buffer A200D. All of the samples were rotated ∼16 h at 4°C, washed five times with 0.5 ml of buffer A200D, and eluted with sample buffer.

For Fig. 4 B, GST-Sec9c (∼180 μg, ∼3.2 nmole) was bound in batch for eight samples as in Fig. 4 A. His_8-Sso1p (∼320 μg, ∼9 nmol) was added, the volume adjusted to 150 μl and incubated ∼15 h at 4°C on a rotating wheel. Unbound Sso1p was removed by five, 0.5 ml washes with buffer A200D. The bound t-SNARE complex was separated into eight aliquots (12.5 μl packed beads) and Sec1p (250 μl, ∼0.4 nmol) was added to four samples and buffer A200D (250 μl) was added to the other four. The incubation continued for 7 h at 4°C on a rotating wheel. Bound complexes were washed five times with buffer A200D and Snc2p was added in increasing amounts (0, ∼0.4, ∼0.8, or 1.6 nmoles) to each of

the eight samples respectively and the total volume of each tube was adjusted to 300 μl. Complexes mixed at 4°C for ~16 h and were washed and eluted as described.

Recombinant Sec1p addition to the fusion assay

Unlabeled t-SNARE liposomes (10 μL, 215 pmoles total protein) were mixed for ~16 h at 4°C with recombinant Sec1p (85 μL, 150 pmoles) or buffer A200 (85 μl). The t-SNARE complex solutions were mixed with Snc1p labeled liposomes (5 μL, 600 pmoles) and fusion was monitored as described previously (Weber et al., 1998; Scott et al., 2003). Soluble Snc2pΔTMD (2 μL, ~660 pmoles) was added to t-SNARE liposomes for 15 min before the addition of the labeled Snc1p liposomes in order to inhibit fusion stimulation and determine the background level of fusion.

Reconstitution in the presence of Sec1p

A twofold dilution series of His_6-Sec1p protein (700, 350, 175, and 87.5 pmoles) in 400 μl total volume or buffer A200 (400 μl) was mixed with His_8-Sso1p (40 μl, 4,715 pmoles) and GST-Sec9c (60 μl, 7,663 pmoles) to form t-SNARE complex in the presence of 0.6% OG. Additionally, Sec1p (700 pmoles) was mixed with Sso1p alone; His_8-Sso1p (40 μL, 4,715 pmoles) and buffer A200 (60 μl). Samples were mixed for 16 h at 4°C and reconstituted into unlabeled lipid as previously described (Scott et al., 2003). Sec1p binding was analyzed by SDS-PAGE (Fig. 6 A). Fusion between Snc1p labeled liposomes and t-SNARE unlabeled liposomes containing Sec1p from 0–700 pmoles was monitored as previously described (Weber et al., 1998; Scott et al., 2003). Soluble Snc2p (2 μl, ~660 pmoles) was added to t-SNARE liposomes containing the highest amount of Sec1p for 15 min before adding the labeled Snc1p liposomes to inhibit stimulation of fusion and determine the background level of fusion. The maximal stimulation of fusion by Sec1p was achieved by adding ~700 pmoles of His_6-Sec1p protein with t-SNARE proteins before reconstitution was tested with four independent preparations of His_6-Sec1p protein. The average fold stimulation with SEM was calculated from these experiments (Fig. 5 C).

Immunofluorescence microscopy

Cell fixation and antibody staining. W30131A transformed with pJM355 was grown at 30°C in synthetic complete media and analyzed by indirect immunofluorescence microscopy by standard methods (Burke et al., 2000) with an anti-Sec1p pAb (RC57; 1:1,000) and an anti-HA mAb (16B12; Covance; 1:1,000) followed by fluorescent secondary antibodies (Alexa Fluor 488 goat anti–mouse IgG and Alexa Fluor 546 goat anti–rabbit IgG [Molecular Probes]) at 1:1,000.

Microscopy. Fluorescent images were taken and analyzed with an Axioplan 2 microscope (Carl Zeiss MicroImaging, Inc.) and a Plan-NEOFLUAR 100× oil-immersion objective (1.3 NA; Carl Zeiss MicroImaging, Inc.) using filter sets for fluorescein (FITC, excitation 480 nm, emission 535 nm, dichroic Q505LP) and Cy3 (excitation 545, emission 610, Dichroic Q570LP) (Chroma Technology Corp.). Images were captured using a CoolSNAP HQ digital camera (Roper Scientific) and MetaMorph Imaging software (version 6.1; Universal Imaging Corp.). The images were deconvolved using the no neighbors algorithm and digitally magnified before assembly with Adobe Photoshop v. 7.0. Several different isolates of the strain were examined to confirm the reproducibility of the observed localization of Sec1p.

Data analysis

Fusion assays were converted to Rounds of Fusion as described previously (Parlati et al., 1999; Scott et al., 2003). Coomassie blue–stained gels were quantified using NIH Image v. 1.63 to generate lane plots of scanned gels and Kaleidigraph (Synergy Software) to integrate peaks.

The authors would like to thank Dr. Fabienne Paumet, Dr. Tom Melia, and Travis Rodkey for thoughtful comments on the manuscript and many helpful suggestions. We also thank Dr. Shunsuke Ishii for the pT-groE plasmid and offer special thanks to Dr. Pat Brennwald for his continued support throughout the years.

This work was supported by grants from the National Science Foundation (IBN-0212605) and The Robert A. Welch Foundation (C-1517) to J.A. McNew, a National Science Foundation IGERT training grant (DGE-0114264; to J. Van Komen), and the Houston Livestock Show and Rodeo (to J. Van Komen and B.L. Scott).

Submitted: 4 May 2004
Accepted: 27 August 2004

References

Banta, L.M., T.A. Vida, P.K. Herman, and S.D. Emr. 1990. Characterization of yeast Vps33p, a protein required for vacuolar protein sorting and vacuole biogenesis. *Mol. Cell. Biol.* 10:4638–4649.

Brennwald, P., B. Kearns, K. Champion, S. Keranen, V. Bankaitis, and P. Novick. 1994. Sec9 is a SNAP-25-like component of a yeast SNARE complex that may be the effector of Sec4 function in exocytosis. *Cell.* 79: 245–258.

Burke, D., D. Dawson, and T. Stearns, and Cold Spring Harbor Laboratory. 2000. Methods in Yeast Genetics: A Cold Spring Harbor Laboratory Course Manual. Cold Spring Harbor Laboratory Press, Cold Spring Harbor. NY. 205 pp.

Carr, C.M., E. Grote, M. Munson, F.M. Hughson, and P.J. Novick. 1999. Sec1p binds to SNARE complexes and concentrates at sites of secretion. *J. Cell Biol.* 146:333–344.

Cowles, C.R., S.D. Emr, and B.F. Horazdovsky. 1994. Mutations in the VPS45 gene, a SEC1 homologue, result in vacuolar protein sorting defects and accumulation of membrane vesicles. *J. Cell Sci.* 107:3449–3459.

Dresbach, T., M.E. Burns, V. O'Connor, W.M. DeBello, H. Betz, and G.J. Augustine. 1998. A neuronal Sec1 homolog regulates neurotransmitter release at the squid giant synapse. *J. Neurosci.* 18:2923–2932.

Dulubova, I., S. Sugita, S. Hill, M. Hosaka, I. Fernandez, T.C. Sudhof, and J. Rizo. 1999. A conformational switch in syntaxin during exocytosis: role of munc18. *EMBO J.* 18:4372–4382.

Dulubova, I., T. Yamaguchi, Y. Gao, S.W. Min, I. Huryeva, T.C. Sudhof, and J. Rizo. 2002. How Tlg2p/syntaxin 16 "snares" Vps45. *EMBO J.* 21:3620–3631.

Fiebig, K.M., L.M. Rice, E. Pollock, and A.T. Brunger. 1999. Folding intermediates of SNARE complex assembly. *Nat. Struct. Biol.* 6:117–123.

Finger, F.P., T.E. Hughes, and P. Novick. 1998. Sec3p is a spatial landmark for polarized secretion in budding yeast. *Cell.* 92:559–571.

Fukuda, R., J.A. McNew, T. Weber, F. Parlati, T. Engel, W. Nickel, J.E. Rothman, and T.H. Sollner. 2000. Functional architecture of an intracellular membrane t-SNARE. *Nature.* 407:198–202.

Gallwitz, D., and R. Jahn. 2003. The riddle of the Sec1/Munc-18 proteins - new twists added to their interactions with SNAREs. *Trends Biochem. Sci.* 28:113–116.

Graham, M.E., A.W. Sudlow, and R.D. Burgoyne. 1997. Evidence against an acute inhibitory role of nSec-1 (munc-18) in late steps of regulated exocytosis in chromaffin and PC12 cells. *J. Neurochem.* 69:2369–2377.

Grote, E., C.M. Carr, and P.J. Novick. 2000. Ordering the final events in yeast exocytosis. *J. Cell Biol.* 151:439–452.

Hu, K., J. Carroll, S. Fedorovich, C. Rickman, A. Sukhodub, and B. Davletov. 2002. Vesicular restriction of synaptobrevin suggests a role for calcium in membrane fusion. *Nature.* 415:646–650.

Kosodo, Y., Y. Noda, H. Adachi, and K. Yoda. 2002. Binding of Sly1 to Sed5 enhances formation of the yeast early Golgi SNARE complex. *J. Cell Sci.* 115:3683–3691.

Kosodo, Y., Y. Noda, H. Adachi, and K. Yoda. 2003. Cooperation of Sly1/SM-family protein and sec18/NSF of *Saccharomyces cerevisiae* in disassembly of cis-SNARE membrane-protein complexes. *Biosci. Biotechnol. Biochem.* 67:448–450.

McNew, J.A., J.G. Coe, M. Sogaard, B.V. Zemelman, C. Wimmer, W. Hong, and T.H. Sollner. 1998. Gos1p, a *Saccharomyces cerevisiae* SNARE protein involved in Golgi transport. *FEBS Lett.* 435:89–95.

McNew, J.A., T. Weber, D.M. Engelman, T.H. Sollner, and J.E. Rothman. 1999. The length of the flexible SNAREpin juxtamembrane region is a critical determinant of SNARE-dependent fusion. *Mol. Cell.* 4:415–421.

McNew, J.A., F. Parlati, R. Fukuda, R.J. Johnston, K. Paz, F. Paumet, T.H. Sollner, and J.E. Rothman. 2000a. Compartmental specificity of cellular membrane fusion encoded in SNARE proteins. *Nature.* 407:153–159.

McNew, J.A., T. Weber, F. Parlati, R.J. Johnston, T.J. Melia, T.H. Sollner, and J.E. Rothman. 2000b. Close is not enough: SNARE-dependent membrane fusion requires an active mechanism that transduces force to membrane anchors. *J. Cell Biol.* 150:105–117.

Melia, T.J., T. Weber, J.A. McNew, L.E. Fisher, R.J. Johnston, F. Parlati, L.K. Mahal, T.H. Sollner, and J.E. Rothman. 2002. Regulation of membrane fusion by the membrane-proximal coil of the t-SNARE during zippering of SNAREpins. *J. Cell Biol.* 158:929–940.

Misura, K.M., R.H. Scheller, and W.I. Weis. 2000. Three-dimensional structure of the neuronal-Sec1-syntaxin 1a complex. *Nature.* 404:355–362.

Mumberg, D., R. Muller, and M. Funk. 1995. Yeast vectors for the controlled expression of heterologous proteins in different genetic backgrounds. *Gene.* 156:119–122.

Munson, M., and F.M. Hughson. 2002. Conformational regulation of SNARE

assembly and disassembly in vivo. *J. Biol. Chem.* 277:9375–9381.

Novick, P., C. Field, and R. Schekman. 1980. Identification of 23 complementation groups required for post-translational events in the yeast secretory pathway. *Cell.* 21:205–215.

Ossig, R., C. Dascher, H.H. Trepte, H.D. Schmitt, and D. Gallwitz. 1991. The yeast SLY gene products, suppressors of defects in the essential GTP-binding Ypt1 protein, may act in endoplasmic reticulum-to-Golgi transport. *Mol. Cell. Biol.* 11:2980–2993.

Parlati, F., T. Weber, J.A. McNew, B. Westermann, T.H. Sollner, and J.E. Rothman. 1999. Rapid and efficient fusion of phospholipid vesicles by the alpha-helical core of a SNARE complex in the absence of an N-terminal regulatory domain. *Proc. Natl. Acad. Sci. USA.* 96:12565–12570.

Parlati, F., J.A. McNew, R. Fukuda, R. Miller, T.H. Sollner, and J.E. Rothman. 2000. Topological restriction of SNARE-dependent membrane fusion. *Nature.* 407:194–198.

Parlati, F., O. Varlamov, K. Paz, J.A. McNew, D. Hurtado, T.H. Sollner, and J.E. Rothman. 2002. Distinct SNARE complexes mediating membrane fusion in Golgi transport based on combinatorial specificity. *Proc. Natl. Acad. Sci. USA.* 99:5424–5429.

Paumet, F., B. Brugger, F. Parlati, J.A. McNew, T.H. Sollner, and J.E. Rothman. 2001. A t-SNARE of the endocytic pathway must be activated for fusion. *J. Cell Biol.* 155:961–968.

Paumet, F., V. Rahimian, and J.E. Rothman. 2004. The specificity of SNARE-dependent fusion is encoded in the SNARE motif. *Proc. Natl. Acad. Sci. USA.* 101:3376–3380.

Peng, R., and D. Gallwitz. 2002. Sly1 protein bound to Golgi syntaxin Sed5p allows assembly and contributes to specificity of SNARE fusion complexes. *J. Cell Biol.* 157:645–655.

Pfeffer, S.R. 2001. Rab GTPases: specifying and deciphering organelle identity and function. *Trends Cell Biol.* 11:487–491.

Scott, B.L., J.S. Van Komen, S. Liu, T. Weber, T.J. Melia, and J.A. McNew. 2003. Liposome fusion assay to monitor intracellular membrane fusion machines. *Methods Enzymol.* 372:274–300.

Sikorski, R.S., and P. Hieter. 1989. A system of shuttle vectors and yeast host strains designed for efficient manipulation of DNA in *Saccharomyces cerevisiae*. *Genetics.* 122:19–27.

Sollner, T., S.W. Whiteheart, M. Brunner, H. Erdjument-Bromage, S. Geromanos, P. Tempst, and J.E. Rothman. 1993. SNAP receptors implicated in vesicle targeting and fusion. *Nature.* 362:318–324.

TerBush, D.R., T. Maurice, D. Roth, and P. Novick. 1996. The Exocyst is a multiprotein complex required for exocytosis in *Saccharomyces cerevisiae*. *EMBO J.* 15:6483–6494.

Thurmond, D.C., B.P. Ceresa, S. Okada, J.S. Elmendorf, K. Coker, and J.E. Pessin. 1998. Regulation of insulin-stimulated GLUT4 translocation by Munc18c in 3T3L1 adipocytes. *J. Biol. Chem.* 273:33876–33883.

Thurmond, D.C., M. Kanzaki, A.H. Khan, and J.E. Pessin. 2000. Munc18c function is required for insulin-stimulated plasma membrane fusion of GLUT4 and insulin-responsive amino peptidase storage vesicles. *Mol. Cell. Biol.* 20:379–388.

Toonen, R.F., and M. Verhage. 2003. Vesicle trafficking: pleasure and pain from SM genes. *Trends Cell Biol.* 13:177–186.

Tucker, W.C., T. Weber, and E.R. Chapman. 2004. Reconstitution of Ca^{2+}-regulated membrane fusion by synaptotagmin and SNAREs. *Science.* 304: 435–438.

Ungar, D., and F.M. Hughson. 2003. SNARE protein structure and function. *Annu. Rev. Cell Dev. Biol.* 19:493–517.

Voets, T., R.F. Toonen, E.C. Brian, H. de Wit, T. Moser, J. Rettig, T.C. Sudhof, E. Neher, and M. Verhage. 2001. Munc18-1 promotes large dense-core vesicle docking. *Neuron.* 31:581–591.

Weber, T., B.V. Zemelman, J.A. McNew, B. Westermann, M. Gmachl, F. Parlati, T.H. Söllner, and J.E. Rothman. 1998. SNAREpins: minimal machinery for membrane fusion. *Cell.* 92:759–772.

Wu, M.N., J.T. Littleton, M.A. Bhat, A. Prokop, and H.J. Bellen. 1998. ROP, the *Drosophila* Sec1 homolog, interacts with syntaxin and regulates neurotransmitter release in a dosage-dependent manner. *EMBO J.* 17:127–139.

Yamaguchi, T., I. Dulubova, S.W. Min, X. Chen, J. Rizo, and T.C. Sudhof. 2002. Sly1 binds to Golgi and ER syntaxins via a conserved N-terminal peptide motif. *Dev. Cell.* 2:295–305.

Yang, B., M. Steegmaier, L.C. Gonzalez Jr., and R.H. Scheller. 2000. nSec1 binds a closed conformation of syntaxin1A. *J. Cell Biol.* 148:247–252.

Yasukawa, T., C. Kanei-Ishii, T. Maekawa, J. Fujimoto, T. Yamamoto, and S. Ishii. 1995. Increase of solubility of foreign proteins in *Escherichia coli* by coproduction of the bacterial thioredoxin. *J. Biol. Chem.* 270:25328–25331.